Semester report

by Botond OSVÁTH (botond.osvath@ttk.elte.hu)

PhD Program: Statistical Physics, Biological Physics and Physics of Quantum Systems

Supervisors: László OROSZLÁNY and Gergely BARCZA

Ph.D. Thesis title: Investigation of topological superconductors in the presence of interactions

1 Research work carried out in current semester

My main goal for this semester was to complete my first article about the $\mathbb{Z}_4$ parafermion model I've been working on in the previous 2 semesters and publish it.

1.1 $\mathbb{Z}_4$ parafermion model

1.1.1 Local quantities

The expectation value of the local electron density $n_{m,\zeta} = \sum_s c^\dagger_{m,\zeta,s} c_{m,\zeta,s}$, as confirmed by my calculations, is the same for all four states, while the matrix element between two distinct states is exactly zero.

However, introducing a local magnetic field that breaks time-reversal symmetry results in the degeneracy of the ground state being lifted. For example, as depicted in Figure 1 (a) and (b), the expectation value of the local spin momentum $S^y_{m\zeta}$ in the even subspace is highly localized to the region with interactions, but it exhibits a sign difference for the two states. The other matrix elements associated with the local spin operators were determined to be negligible. A similar trend is observed in the odd subspace. This pattern of magnetization displayed by the ground state manifold is a direct outcome of the interaction used, as it promotes an anisotropic spin configuration.

Single-particle excitations with zero energy within the ground state manifold exhibit exponential localization at the interfaces between the superconducting and interacting regions, as illustrated in Figure 1 (c). This observation serves as evidence for the presence of two parafermionic zero modes associated with the boundary of the interacting region.

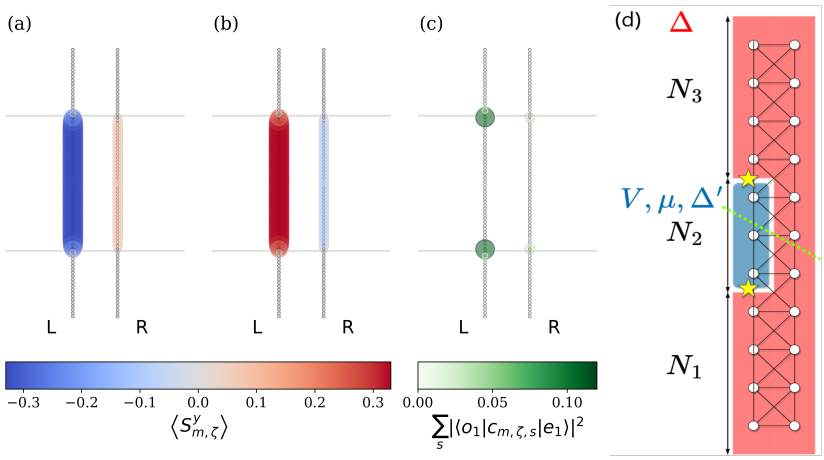

Figure 1: Different local quantities evaluated in the fourfold degenerate subspace with $V/t = 2.2$ and $\Delta' = \mu = 0$ for a setup shown in (d) with lengths $N_1 = N_3 = 20$ and $N_2 = 40$. (a) and (b) depicts the expectation value of the local spin momentum $\langle e_1 | S^y_{m,\zeta} | e_1 \rangle$ and $\langle e_2 | S^y_{m,\zeta} | e_2 \rangle$ in the even subspace. The states in the odd subspace, $|o_1\rangle$ and $|o_1\rangle$, show the same pattern up to numerical precision. (c) shows the matrix element $\sum_s |\langle o_1 | c_{m,\zeta,s} | e_1 \rangle|^2$ of the local annihilation operator $c_{m,\zeta,s}$ between states of the even and odd subspace.

1.1.2 Isotropic Heisenberg interaction

We can replace the previously introduced interaction with the following, isotropic Heisenberg interaction:

$$H_{\text{int}} = \sum_{m,\zeta} \left(J_{m,\zeta} \mathbf{S}_{m,\zeta} \cdot \mathbf{S}_{m+1,\zeta} + A_{m,\zeta} S^x_{m,\zeta} S^x_{m+1,\zeta} \right), \tag{1}$$

where $J_{m,\zeta}$ is the strength of isotropic Heisenberg exchange, $A_{m,\zeta}$ is the single axis anisotropy's strength with $\mathbf{S}_{m,\zeta} = (S^x_{m,\zeta}, S^y_{m,\zeta}, S^z_{m,\zeta})$ being the electron spin vector. This specific form of interaction is especially relevant from an experimental point of view, as it can be realized in a laboratory.

The phase diagram of the model is shown in Figure 2. In this phase diagram, for sufficiently large negative J, two phases (separated by a critical line) with small entanglement entropy can be identified.

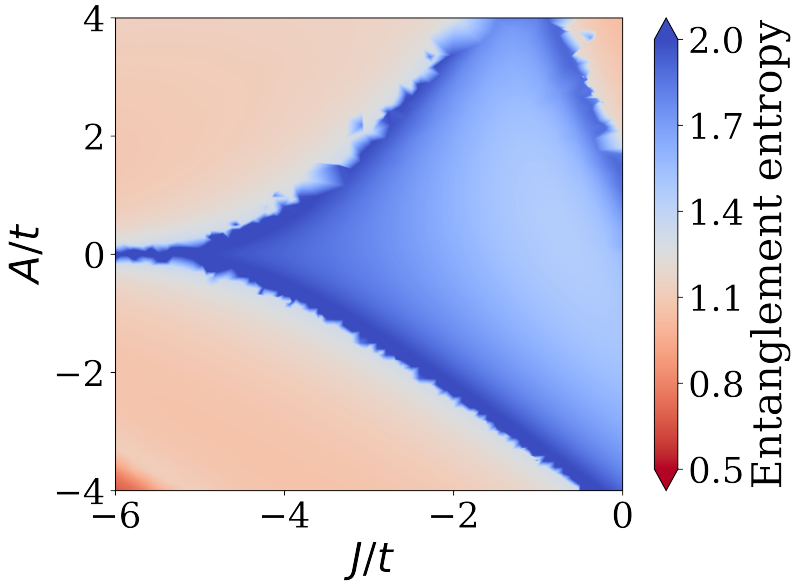

Figure 2: Phase diagram for isotropic exchange J and anisotropic exchange A.

The excitation spectrum evaluated at $J/t = -4$ can be seen in Figure 3. It shows that the previously mentioned two regions are characterized by a fourfold degenerate ground state, and they have a considerable excitation gap. At around zero anisotropy ($A = 0$), the two phases are separated by a metallic critical region. Further numerical investigation shows that the two low-entropy regions are characterized by a parafermionic 8π periodic Josephson spectrum.

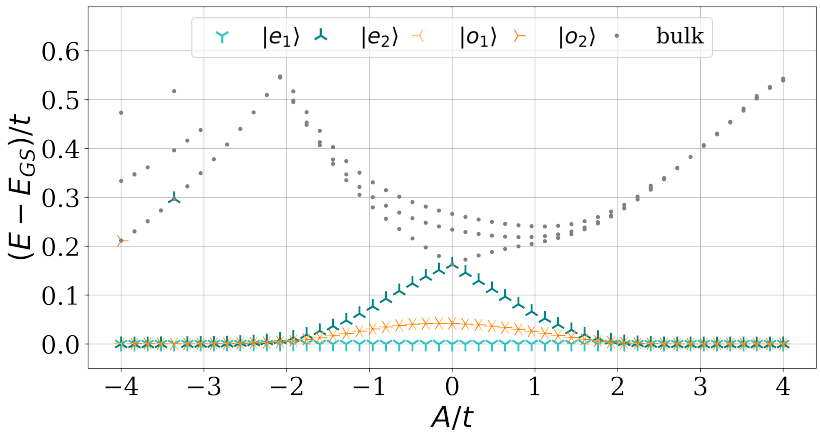

Figure 3: Excitation spectrum as the function of the anisotropic exchange A for $J = -4t$.

1.2 Newly started work

1.2.1 New model, new parafermions

Finding $\mathbb{Z}_4$ parafermions is a great step, but I can go further. In general, $\mathbb{Z}_d$ parafermions for odd d make it possible to generate the full Clifford group, while it is suspected that only a subset of them is realizable for even d. Furthermore, for prime values of d, it is possible to create a two-qubit gate that is independent of the Clifford group by having two parafermion modes interacting [1]. This makes parafermions with prime $d > 2$ sufficient for universal quantum computing. The next step was to look for new models to examine, in the hope of finding $\mathbb{Z}_3$ parafermions.

Discovering $\mathbb{Z}_4$ parafermions represents a significant advancement, yet there is potential for further exploration. Generally, the existence of $\mathbb{Z}_d$ parafermions for odd values of d enables the generation of the entire Clifford group, while it is suspected that only a subset is possible in the case of even d. Notably, for prime values of d, the ability to construct a two-qubit gate independent of the Clifford group is feasible through the interaction of two parafermion modes [1]. Consequently, parafermions with prime $d > 2$ prove sufficient for achieving universal quantum computing. Subsequently, my focus shifted towards the identification of novel models to uncover $\mathbb{Z}_3$ parafermions.

A promising model is depicted in Figure 4, showing two Rashba QWs coupled to an s-wave superconductor [2].

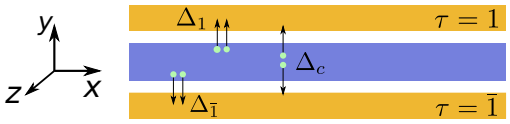

Figure 4: A sketch of a system of two Rashba QWs coupled to an s-wave superconductor, from [2].

The following lattice Hamiltonian can model the system:

$$H = H_{\text{kin}} + H_{\text{sc}} + H_{\text{Rhasba}} + H_{\text{Hubbard}}, \tag{2}$$

where

$$H_{\text{kin}} = t \sum_{n=1}^{N-1} \sum_{\tau=\pm 1} \sum_{\sigma=\uparrow,\downarrow} \left(a^\dagger_{n+1,\tau,\sigma} a^\dagger_{n,\tau,\sigma} + a^\dagger_{n,\tau,\sigma} a^\dagger_{n+1,\tau,\sigma} \right) - \mu \sum_{n=1}^{N} \sum_{\tau=\pm 1} \sum_{\sigma=\uparrow,\downarrow} a^\dagger_{n,\tau,\sigma} a^\dagger_{n,\tau,\sigma} \tag{3}$$

with real hopping parameter t and chemical potential μ,

$$H_{\text{sc}} = \sum_{n=1}^{N} \sum_{\tau=\pm 1} \left(\Delta_\tau \left(a_{n,\tau,\uparrow} a_{n,\tau,\downarrow} + a^\dagger_{n,\tau,\downarrow} a^\dagger_{n,\tau,\uparrow} \right) + \Delta_c \left(a_{n,\tau,\uparrow} a_{n,\bar{\tau},\downarrow} + a^\dagger_{n,\bar{\tau},\downarrow} a^\dagger_{n,\tau,\uparrow} \right) \right) \tag{4}$$

with real superconductivity parameters Δ_1 and $\Delta_{\bar{1}}$ for same-wire and Δ_c for opposite-wire effect,

$$H_{\text{Rhasba}} = i \sum_{n=1}^{N-1} \sum_{\tau=\pm 1} \sum_{\sigma=\uparrow,\downarrow} \left(\alpha_\tau \sigma \left(a^\dagger_{n+1,\tau,\sigma} a^\dagger_{n,\tau,\sigma} - a^\dagger_{n,\tau,\sigma} a^\dagger_{n+1,\tau,\sigma} \right) \right) \tag{5}$$

with real δ_1 and $\delta_{\bar{1}}$ coupling parameters and $\uparrow = 1$, $\downarrow = -1$ convention and

$$H_{\text{Hubbard}} = U \sum_{n=1}^{N} \sum_{\tau=\pm 1} n^\dagger_{n,\tau,\uparrow} n^\dagger_{n,\tau,\downarrow} \tag{6}$$

with real Hubbard parameter U.

1.2.2 Speeding up the calculations

My work would benefit from an improved calculation method, as a significant part of my research is to calculate the eigenfunctions (and other physical quantities) of Hamiltonians. I started to look into two different solutions: the GPU-accelerated ITensor [3] and the Budapest DMRG algorithm (both the CPU and GPU version) [4]. Generally speaking, GPU acceleration can speed up large matrix operations by magnitudes (this ranges, of course, on a great spectrum), and that is exactly what DMRG does under the hood [5]. This work is in the early stages, so I cannot draw any conclusions at the moment.

2 Publications

My first paper, titled "A simple electronic ladder model harboring $\mathbb{Z}_4$ parafermions" is currently submitted to Physical Review Letters and is under referee review. It is already available on arXiv [6].

My research was also featured in KIFÜ's HPC Echo magazine [7].

3 Studies in current semester

I attended three classes in the current semester:

- "Klasszikus és kvantumoptimalizáció" (subject code: "FIZ/3/097")
- "Adatmodellek és adatbázisok a tudományban" (subject code: "FIZ/3/086")
- "Soktestprobléma II." (subject code: "FIZ/1,3/050E")

4 Conferences in current semester

In the current semester, I haven't attended any conferences.

5 Teaching activity in current semester

In the current semester, I participated as a lecturer (for 1 class/week, i.e. 2 hours/week) in the practice class "Számítógépes alapismeretek" (with subject code "szamalapf19la"), which is an introductory course into Linux basics, LaTeX, and Python for first-semester Physics BSc students.

6 Acknowledgements

My research was supported by the Ministry of Innovation and Technology and the National Research, Development and Innovation Office within the Quantum Information National Laboratory of Hungary.

I acknowledge KIFÜ for awarding me access to computational resources based in Hungary.

References

[1] Adrian Hutter and Daniel Loss. Quantum computing with parafermions. *Phys. Rev. B*, 93:125105, Mar 2016.

[2] Jelena Klinovaja and Daniel Loss. Time-reversal invariant parafermions in interacting rashba nanowires. *Phys. Rev. B*, 90:045118, Jul 2014.

[3] Matthew Fishman, Steven R. White, and E. Miles Stoudenmire. The ITensor software library for tensor network calculations, 2020.

[4] Örs Legeza, Libor Veis, and Tamas Mosoni. QC-DMRG-Budapest, a program for model and ab initio DMRG calculations, 2020.

[5] Andor Menczer and Örs Legeza. Boosting the effective performance of massively parallel tensor network state algorithms on hybrid cpu-gpu based architectures via non-abelian symmetries, 2023.

[6] Botond Osváth, Gergely Barcza, Örs Legeza, Balázs Dóra, and László Oroszlány. A simple electronic ladder model harboring $\mathbb{Z}_4$ parafermions, 2023.

[7] KIFÜ. HPC Echo 2022-2023. `https://hpc.kifu.hu/sites/default/files/2023-11/HPC_Echo_2023_hu_fin.pdf`, 2023. Accessed on January 1, 2024.